

BUILDING STRUCTURE MONITORING WITH A FIBRE BRAGG GRATINGS SENSOR

Emil SMEU¹,
Harald GNEWUCH², David JACKSON²,
Adrian PODOLEANU²

Abstract. *The distance changes between structural elements inside a building (e.g. walls, pillars, stairs, etc.) ought to be monitored, especially in seismic-prone areas, in order to assess its stability. Fibre Bragg grating (FBG) sensors are now the most interesting choice for this purpose, since several gratings can be included in the fibre, resulting in a quasi-distributed sensor, which can be illuminated using a single light source and interrogated simply by a single optical spectrum analyser (OSA).*

The paper deals with such a sensor, which was installed for monitoring the distance changes in a construction joint between two building blocks inside the University "Politehnica" of Bucharest. Since this city is placed in a seismic-prone area, we use a fast scanning OSA, so that the dynamic behaviour of the monitored construction joint is expected to be captured during future earthquakes. Slow drifts of the construction joint width will be also monitored.

The paper describes the sensor structure and working principle, the experimental tests and main parameters evaluation. The reported sensor is temperature compensated.

Keywords: FBG, temperature compensation, strain, calibration tests

1. Introduction

Civil engineers are interested to know in detail the buildings vibrational behaviour during earthquakes. Slow drifts in distance between structural elements of the building and induced strains are also of great interest. For this purpose, FBG sensors are ideal due to their capability of being easily embedded (smart structure) or surface mounted and their ease of interrogation. Advanced FBG strain sensors were reported as early as 1992 [1], and then structural monitoring for buildings and bridges using FBGs became a constant concern for researchers [2-6].

The paper reports on a simple FBG sensor, which monitors the distance changes in a construction joint between two building blocks inside the University "Politehnica" of Bucharest and which has the capability of covering a wide displacement range of up to +/- 20 mm. This sensor is temperature compensated.

¹University "Politehnica" of Bucharest, Physics Dept., 313, Spl. Independentei, Bucharest 060042, Romania (emil_smeu@physics.pub.ro).

²University of Kent, School of Physical Sciences, Applied Optics Group, Canterbury CT2 7NR, UK.

2. Theory of operation

A piece of bare fibre which includes a FBG (fusion spliced) is fixed in two points, each on the sides of the monitored construction joint.

When the buildings tilt relative to each other, the width of the joint changes, resulting in the fibre to be stretched.

The induced strain leads to a change in the pitch of the FBG which in turn leads to a change of the reflected wavelength when the FBG is illuminated along its axis with a broadband light source, here a superluminescent diode (SLD).

From the study of scientific literature the dynamic range of the strain in the FBG to be measured is between $S = 1 \mu\epsilon$ and $5 \text{ m}\epsilon$, with S being the strain, defined by:

$$S = \frac{\Delta l}{l_0} \quad (1)$$

with Δl and l_0 being the elongation and initial length, respectively.

Here, the lower value of the dynamic range describes the detection limit of strain using FBGs whereas the higher value is the maximum strain of a silica fibre which can sustain over a long time without breaking.

The task was to find a topology of the displacement sensor, for a reasonable sensor size, so that the dynamic range of the horizontal displacement of $\pm 20 \text{ mm}$ falls within the dynamic range of the strain for the optical fibre.

This can be accomplished by the following arrangement, as illustrated in Fig. 1.

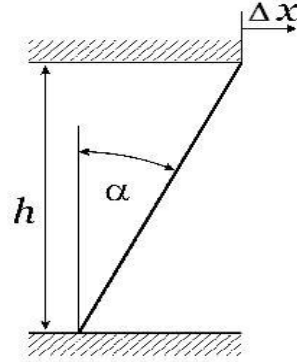


Fig. 1. Topology of displacement sensor using FBGs.

Using simple geometry the following dependency of the strain S on height h , horizontal displacement Δx , and initial inclination angle α of the optical fibre can be derived:

$$S(\Delta x, h, \alpha) = -1 + \sqrt{1 + \frac{\Delta x}{h} \sin(2\alpha) + \left(\frac{\Delta x}{h}\right)^2 \cos^2 \alpha} \quad (2)$$

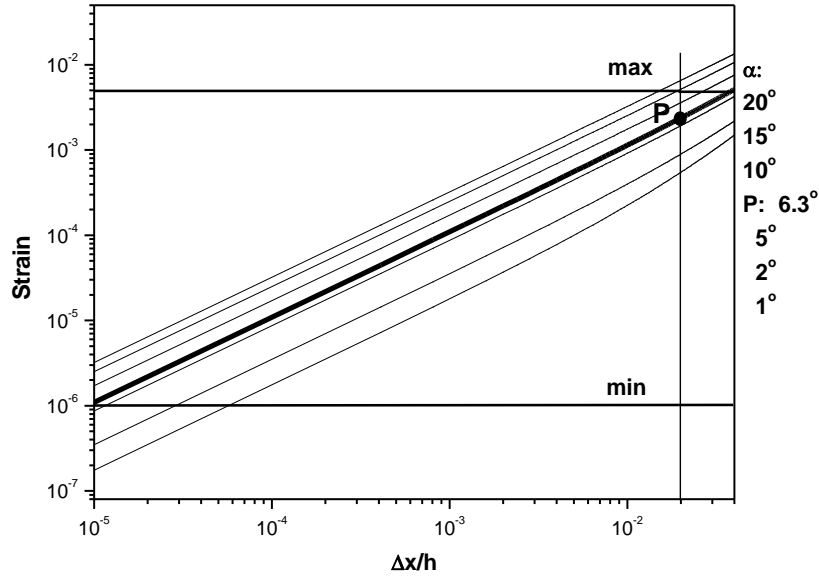


Fig. 2. Induced strain vs. normalized horizontal displacement $\Delta x/h$ and inclination angle α .

Fig. 2 displays equation (2). The strain limits are shown by two horizontal lines. From this one can deduce that for $h = 1$ m and an inclination angle α between 5° and 10° , the horizontal displacement over its entire dynamic range can be monitored. We have used an angle of 6.3° ($x = 11$ cm). The curve for $\alpha = 6.3^\circ$ is represented with a thick line, and point P corresponds to the set pre-stretching of the fibre, which leads to the dynamic range of ± 20 mm. Although the monitored construction joint is only 1–2 mm wide, and a non-symmetrical dynamic range of $-2 \dots +38$ mm would have been possible, the ± 20 mm dynamic range was preferred, as it corresponds to a higher strain S , which is needed for higher frequency bandwidth, in order to cover the spectrum useful in seismology. The resonance frequency f_1 of the fundamental flexural standing wave of the fibre string is:

$$f_1 = \frac{C}{2L} \sqrt{\frac{ES}{\rho}} \quad (3)$$

where C is constant depending on the polymer jacket protecting the fibre ($C = 1$ for a bare fibre), E is Young's modulus, ρ is the density of silica, and L is the actual fibre string length. Since the useful bandwidth is much smaller than f_1 , which depends on the applied strain.

Of course, there is a simpler topology, namely having the fibre collinear with the displacement vector. The required fibre length would be $l = 20 \text{ mm}/5 \text{ m}\epsilon = 4$ m, resulting in an impractical topology, hence not further considered. Moreover, as the length of the sensing fibre is inversely proportional to its vibration frequency, this simpler topology would reduce the available bandwidth drastically.

3. Sensor architecture

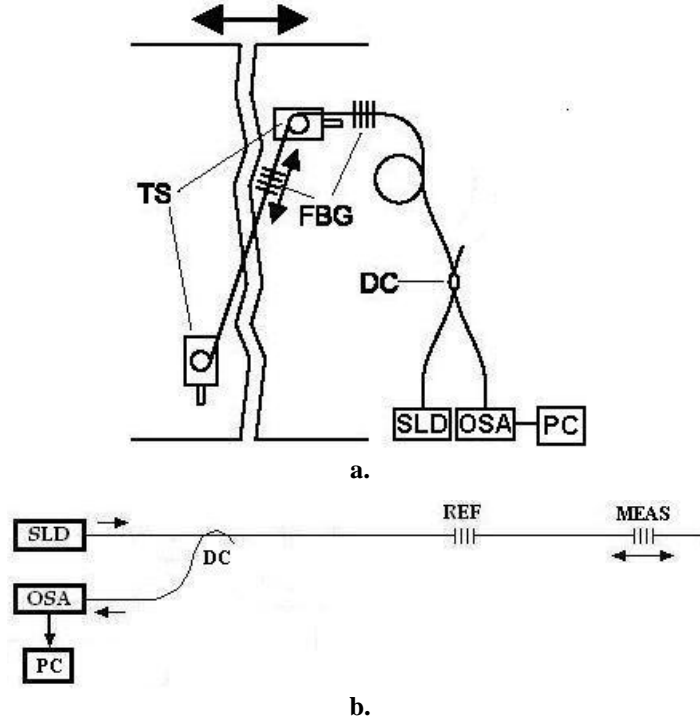


Fig. 3. The setup for monitoring a construction joint between two building blocks at the University “Politehnica” of Bucharest.

a: setup;

b: schematic. DC: 1×2 directional coupler, TS: translation stages (for pre-stretching and calibration), SLD: superluminescent diode, OSA: optical spectrum analyzer, PC: personal computer.

The FBG sensor is composed of two Bragg gratings, of which one is pre-stretched over the monitored construction joint and represents the measurement grating, whereas the other one is not strained and thus used as a reference grating. The use of two identical FBGs (from the same batch) makes the overall measurement nominally insensitive to ambient temperature. The experimental setup is represented in Fig. 3.

The suspended fibre which contains the measurement grating is about 1 m long (actually $h = 1$ m), and the reference FBG is placed near the sensing FBG (so that they are at the same temperature). Both fibres (containing the Bragg gratings) are protected against air currents by a transparent plexiglass box. The illumination source used is an SLD with a center wavelength of 825 nm and a spectral width of 24.1 nm (FWHM), Model SLD 381 10 DIP SM (Superlum Ltd., Moscow). The FBGs have a Bragg wavelength [7] of 811.2 nm in the unstrained case. Both FBGs reflect light which is coupled into the fast scanning OSA via a 1×2 directional coupler.

Fortunately, the amount of optical feedback into the SLD is small, so an optical isolator was not needed. The Bragg wavelength of the pre-stretched FBG increases (decreases) proportionally when the monitored construction joint width increase (decrease). The OSA (Ocean Optics Model USB2000) reveals two spectral peaks for the two FBGs. A spectral scan containing the SLD spectrum and the two reflected peaks is represented in Fig. 4.

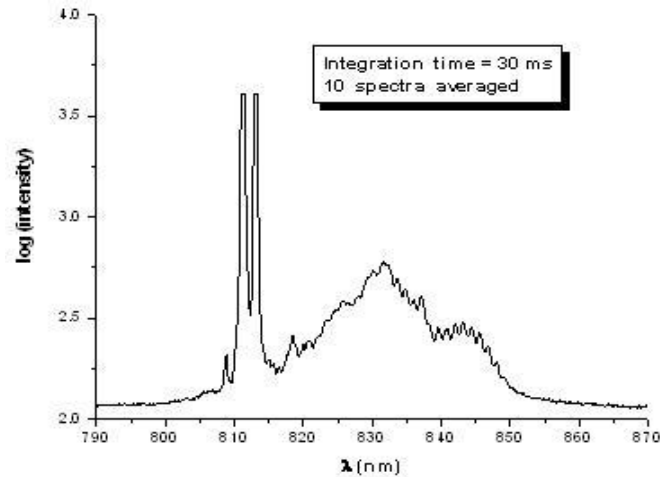


Fig. 4. Reflected lines saturated for observable SLD spectrum.

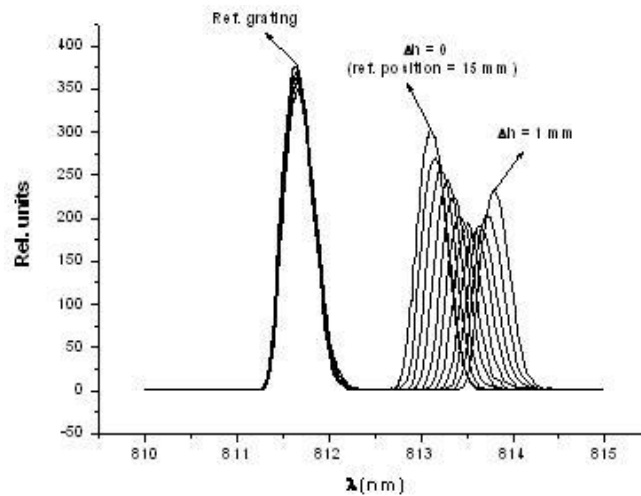


Fig. 5. Spectrograms obtained for 10 values of h (step $\Delta h = 0.1$ mm).

The peak corresponding to the reference FBG depends only on the ambient temperature. The sensing FBG peak depends on the strain and temperature. The wavelength difference of the two peaks is proportional only to the strain, i.e. to the monitored construction joint width. The fixing points of the measurement grating are placed on the two building blocks and their position was tuned with two manual translation stages (fixed on the walls).

The lower translation stage has a movement resolution of 10 μm in the vertical direction, and it was used to pre-stretch the FBG strain sensor (~ 1 mstrain). Using first this stage, the height of the fibre was increased in 10 steps of 0.1 mm and the effect can be seen in Fig. 5. It can be readily seen that the wavelength reflected by the reference FBG remained unchanged, while the peak reflected by the sensing FBG varied according to its strain.

4. Sensor calibration

The calibration plot obtained when changing h as described above is represented in Fig. 6.

We assume that the angle of the sensing FBG in respect to the vertical direction is nearly constant while the width of the monitored construction joint (Δx in equation (2)) changes. This assumption is good enough since the size changes are small compared to the triangle dimensions in Fig. 1 and the approximate relation is valid:

$$\Delta x = \Delta h \times \text{ctg } \alpha \quad (4)$$

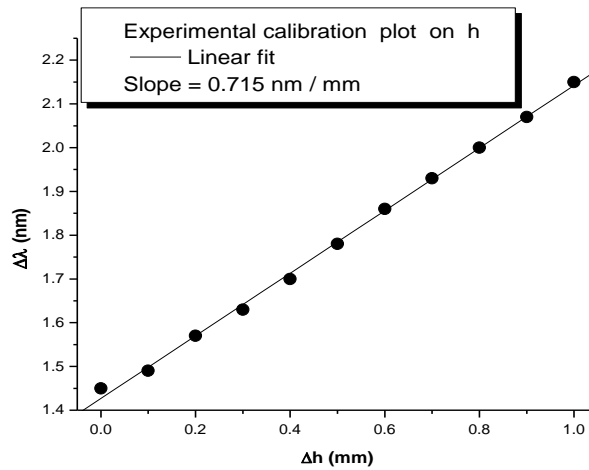


Fig. 6. Calibration plot on h obtained experimentally.

The important parameter in Fig. 7 is the sensor **sensitivity**, which has the value **0.079 nm/mm**. This value was verified experimentally by moving the upper translation stage, which is identical to the lower one (same resolution) in 0.25 mm steps. Fig. 8 resulted. The identity between the calculated sensor sensitivity and the experimental one is remarkable.

In order to determine experimentally the sensor resolution, we have performed a test in which x was changed with a 50 μm , and another with monotonically increasing steps: 10, 20, 30, ..., 100 μm . The variable steps test is represented in Fig. 9. From this figure it seems that **the sensor resolution for displacement detection is at least as good as 10 μm** .

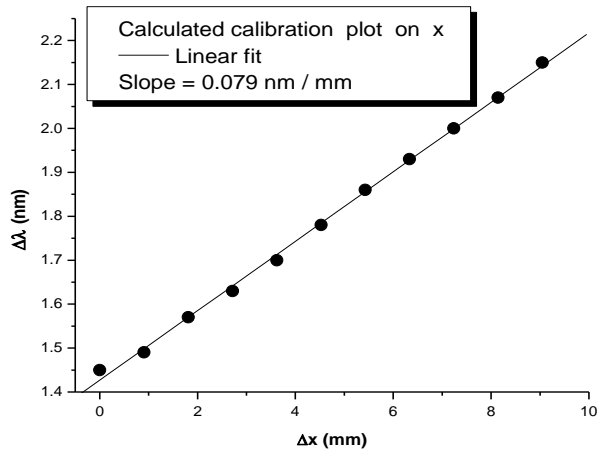


Fig. 7. Calibration plot on x calculated from the one on h via relation (4).

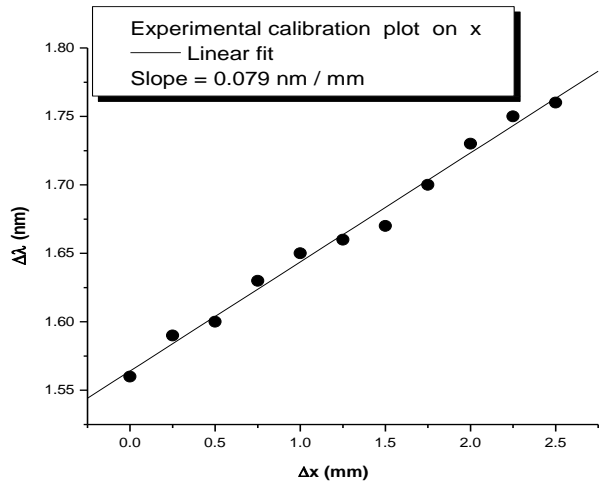


Fig. 8. Calibration plot on x obtained experimentally by changing x with steps of 0.25 mm.

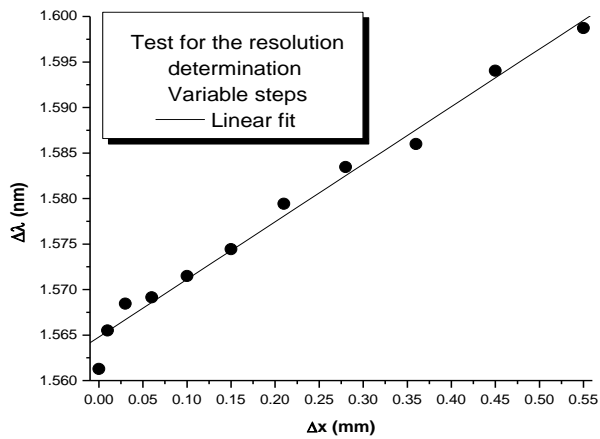


Fig. 9. Static test with variable Δx steps: 10, 20, 30, ..., 100 μ m.

All the wavelengths were calculated by fitting the data points within each peak with Gaussians and determining their maxima, like in Fig. 10.

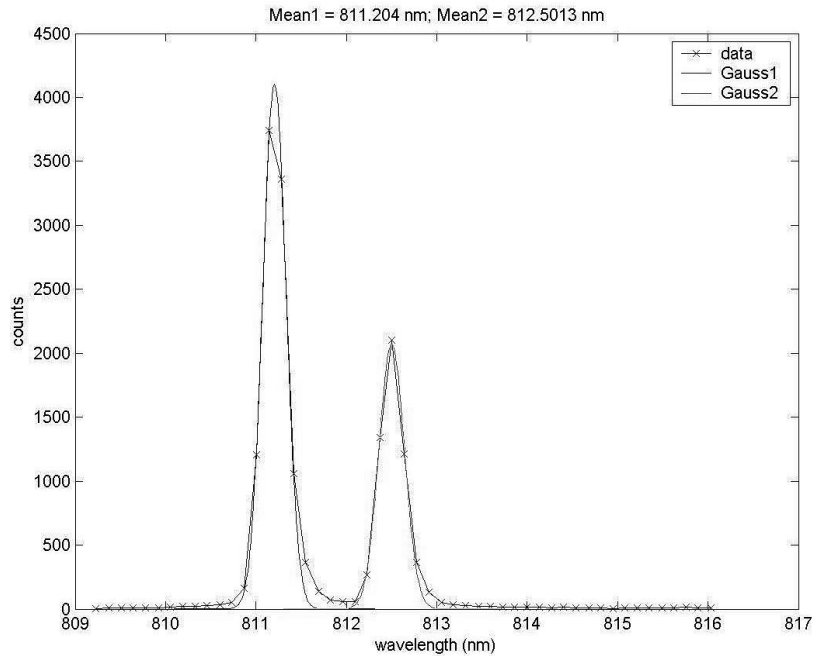


Fig. 10. Peaks wavelengths determination.

The **linearity** of the sensor was determined within the tests with 50 μm and variable steps – see Fig. 11. A **linearity better than +0.2%...-0.35%** was obtained.

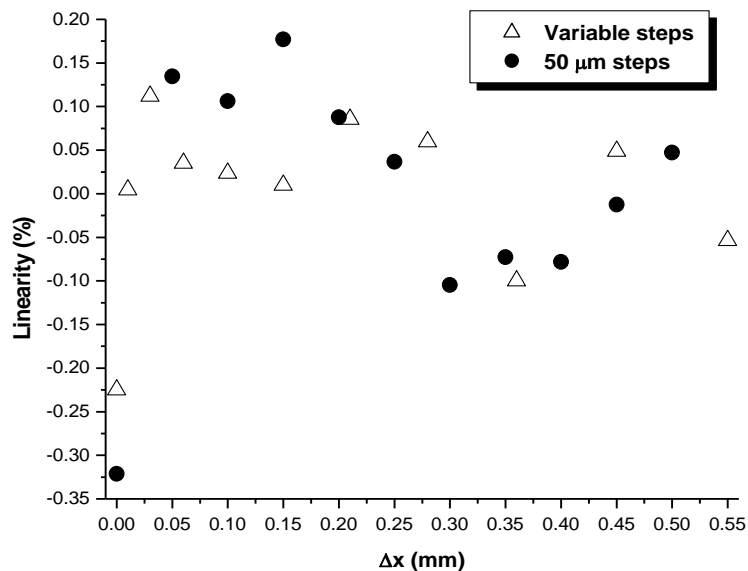


Fig. 11. Determined linearity of the sensor.

5. Dynamic tests

We have also performed dynamic tests, by changing x quasi-periodically, in order to check the sensor ability to “see” movements of the monitored construction joint. Two examples are presented in Figs. 12 and 13.

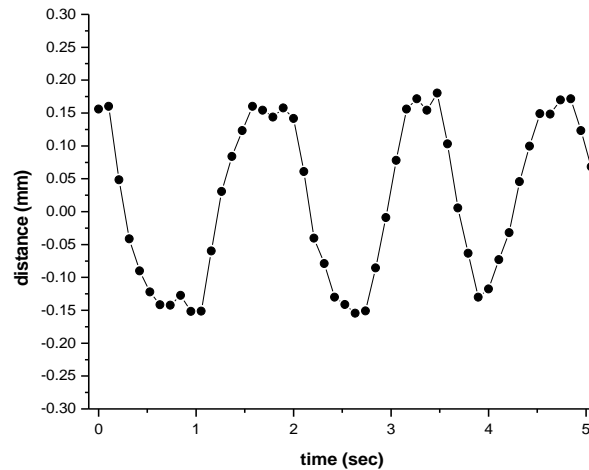


Fig. 12. Dynamic movement test on x with a peak-to-peak amplitude of 0.25-0.3 mm.

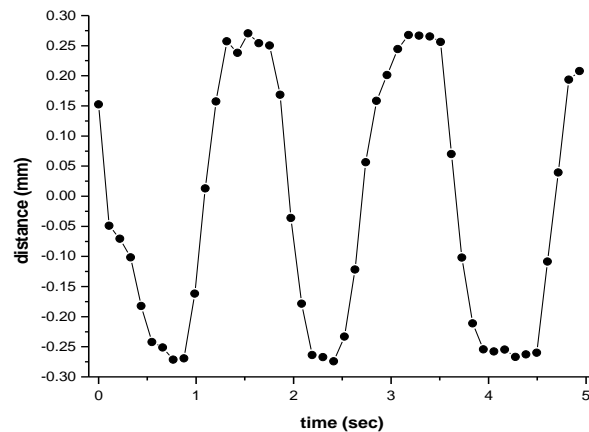


Fig. 13. Dynamic movement test on x with a peak-to-peak amplitude of 0.5-0.6 mm.

6. Conclusions

A FBG sensor for structural building changes is reported, having a much simpler structure and operation than many other sensors^{6,8-10} similar to this one. This was possible due to the use of a CCD array based OSA, to the interrogation software for precise peak wavelengths determination, and to the geometrical desensitisation concept permitting a wide displacement. Moreover, the reported sensor is temperature compensated, unlike many other reported sensors, designed and manufactured for similar purposes.

REFERENCES

- [1] Kersey A. D., Berkoff T. A., and Morey W. W., *High-Resolution Fibre-Grating based Strain Sensor with Interferometric Wavelength-Shift Detection*, Electron. Lett., **28**, pp. 236-238, 1992.
- [2] Dewynter-Marty V., Rougeault S., Ferdinand P., Chauvel D., Toppani E., Leygonie M., Jarret B., and Fenaux P., *Concrete strain measurements and crack detection with surface-mounted and embedded Bragg grating extensometers*, Proc. 12th Int. Conf. on Optical Fiber Sensors, Williamsburg, Optical Society of America, pp. 600-603, 1997.
- [3] Vohra S. T., Todd M. D., Johnson G. A., Chang C. C., and Danver B. A., *Fiber Bragg Grating Sensor System for Civil Structure Monitoring: Applications and Field Tests*, Proc. 13th Int. Conf. on Optical Fiber Sensors, Kyongju, Optical Society of America, pp. 32-37, 1999.
- [4] Shiba K., Kumagai H., Watanabe K., and Iwaki H., *Application technologies of OTDR and FBG Sensors to civil Infrastructures*, Proc. 16th Int. Conf. on Optical Fiber Sensors, Nara, Optical Society of America, pp. 492-495, 2003.
- [5] Udd E., Calvert S., and Kunzler M., *Usage of Fiber Grating Sensors to perform critical Measurements of Civil Infrastructure*, Proc. 16th Int. Conf. on Optical Fiber Sensors, Nara, Optical Society of America, pp. 496-499, 2003.
- [6] J.-G. Liu, C. Schmidt-Hattenberger, G. Borm, *Dynamic strain measurement with a fibre Bragg grating sensor system*, Measurement, **32**, pp. 151-161, 2002.
- [7] Pramod K. Rastogi – Editor, *Optical Measurement Techniques and Applications*, pp. 233, Artech House, Inc., Boston, London, 1997.
- [8] B. Lissak, A. Arie and M. Tur, *High resolution strain sensing by locking lasers to fiber-Bragg gratings*, SPIE Proc. European Workshop on Optical Fibre Sensors, Peebles, Ed.: Brian Culshaw and Julian D. C. Jones, Vol. 3483, pp. 250-254, 1998
- [9] P. J. Moreira, L. A. Ferreira, J. L. Santos and F. Farahi, *Extended Range Interrogation Scheme for Fibre Bragg Grating Sensors Using a Multimode Laser Diode*, SPIE Proc. European Workshop on Optical Fibre Sensors, Peebles, Ed.: Brian Culshaw and Julian D. C. Jones, Vol. 3483, pp. 278-282, 1998.
- [10] Y. Hu, B. Bridge, L. Zhang, I. Bennion, S. Chen, *Improvements on the multiplexing system using a 2D spectrograph for FBG based sensor arrays*, SPIE Proc. European Workshop on Optical Fibre Sensors, Peebles, Ed.: Brian Culshaw and Julian D. C. Jones, Vol. 3483, pp. 288-291, 1998.